

Effect of 3D Printing Parameters on Dimensional Accuracy Using eSteel Filaments

Mahros Darsin¹, Nurcholis Alfian Mahardika¹, Gaguk Jatisukamto¹, Mochamad Edoward Ramadhan¹, Boy Arief Fachri² and Mohd Sabri Hussin³

¹ Department of Mechanical Engineering, Universitas Jember, Indonesia

² Department of Chemical Engineering, Universitas Jember, Indonesia

³ Faculty of Mechanical Technology Engineering, Universiti Malaysia, Malaysia

Received Date: 19-08-2021

Published Date: 16-10-2021

Abstract

3D printing technology or additive manufacturing is manufacturing by adding materials to objects until it is shaped as expected. This technique is easy and cheap for printing polymer-based materials in the form of filament. Recently, some metal-containing filament has been introduced in the market, one of which is eSteel composed of 45% wt. steel and 55% wt. PLA. Due to its premature introduction, it is a minimal published paper discussing its mechanical properties and dimensional accuracy. This research aims to analyze the dimensional accuracy of 3D printed products of the fused deposition modeling (FDM) technique using eSteel filament. Taguchi method was used to design the experiments with orthogonal array L4 (23). There were three control parameters with two levels each, namely extruder temperature (220°C, 225°C), layer height (0.3 mm, 0.4 mm), and raster angle (0°/90°, 45°/45°). These parameters were selected based on initial trials. The specimens are in the form of an ASTM D790 flexural test with five replications in each combination. HE3D K200 3D printing machine was used for printing the filament. Analysis of variance indicated that raster angle has the most influence on dimensional accuracy by 32.09%, followed by extruder temperature with a contribution of 31.72% and layer height by 25.53%. The combination of control parameters to produce optimal dimensional accuracy was obtained when combining parameters: extruder temperature of 220°C, layer height of 0.3 mm, and raster angle of 0°/90°.

Keywords: 3D printing; Taguchi Method; Dimensional Accuracy

Introduction

The first 3D printer was developed by Charles W. Hull (Chuck Hull) in 1984. It was made for prototype design in rapid prototyping, which means it spent a short time manufacturing product, no need to go through a long process and complicated production [1]. This 3D printing technology is also known as additive manufacturing. Additive manufacturing is manufacturing by adding materials to objects until they are shaped as expected [2-3].

Dimensional accuracy is essential for this technology application in the manufacturing sector. The final form of a product determines the appropriateness of a product function. If it does not match the geometric orientation, the product will automatically be rejected. Consequently, it may lead to a detriment for the company. Most of the previous applications of 3D printing were for rapid prototyping. As its name, the printed parts are hopefully in a net or near-net shape of the actual products to reduce further processes and reduce the cost of post-processing. Therefore, the dimensional accuracy of the 3D printed objects is a must. In recent applications, 3D printing has been used for functional objects, such as in medical products for instance bone implants [4-5], construction, and concrete printing [6].

Corresponding author: Mahros Darsin, Mechanical Engineering Department, Universitas Jember, Indonesia

E-mail: mahros.teknik@unej.ac.id

During the 3D printing process, dimensional inaccuracies may occur because the product undergoes a phase change from liquid to solid, decreasing a specific volume on compaction [7]. As a result, there is a shrinkage of the printed component. The main cause of inhomogeneous shrinkage of some parts in the 3D printing process is the delays in solid-ification of the layer, the effect of the geometry of the part, and the effect of the boundary on the surface. Another challenge of 3D printed objects is stair-stepping [8] due to layer-by-layer deposition, which also creates dimensional accuracy.

There are several techniques for 3D printing, one of which is the Fused Deposition Modeling (FDM) technique. FDM is one of the most widely used AM techniques for fabricating polymer components [9]. Currently, there are several filaments for 3D printing with the FDM technique from a mixture of plastic and metal, such as eCopper, eBronze, and eSteel. eSteel is a trademark for filaments for 3D printing feeds. Its composition consists of steel (stainless steel) and plastic (PLA). As a new material with a new composition, very few published papers revealed the mechanical properties and accuracy of the printed products made of it. Sakhtivel investigated the PLA-stainless steel composite filament's tensile strength and impact strength as bio-compatible materials using FDM. They revealed that the maximum tensile strength of the printed part was 69 MPa and toughness of 8 kJ/m² [10]. They suggested further observations on dimensional accuracy and surface finish. This re-search investigates the optimal process parameter settings on 3D printer machines to gain dimensional accuracy using this PLA-steel filament. In addition, a little discussion on flexural strength is presented as a complementary results.

Research Methods

Tools and Materials

The 3D printer machine used HE3D K200 3D. There is no particular reason for utilizing this delta-type printer; it is according to the availability of the machine in the laboratory. In addition, each type of 3D printer should print the object with acceptable precision. A digital caliper of 0.01 mm accuracy was used for measuring the dimension of the product. The filament material used was PLA-stainless steel filament with a composition of 55% wt. PLA and wt. 45% stainless steel, a diameter of 1.75 mm (tolerance of 0.05 mm). Some physical properties of this filament: printing temperature of 200°C-220°C, working bed temperature 25°C-70°C, the density of 2.46 g/cm³. The tools and materials presented in **Figure 1** are as follows.

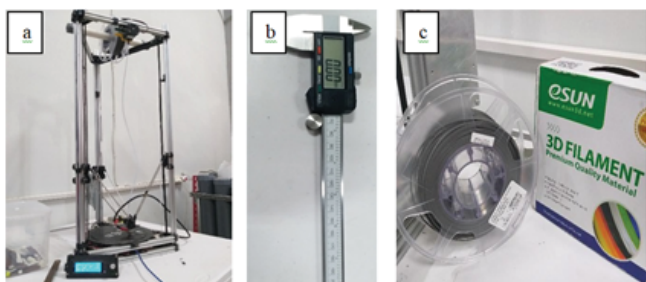


Figure 1: (a) HE3D K200 machine (b) digital caliper (c) eSteel filament.

The control variables in this investigation used 60°C bed temperature, 50 mm/s print speed, rectilinear infill pattern, 100 percent infill density, and 0.6 mm nozzle diameter. The dependent variable in this research is the value of the dimensional accuracy of the test specimen. The independent variables of this study can be seen in **Table 1**.

Parameters	Level 1	Level 2
Extruder temperature (oC)	220	225
Layer height (mm)	0.3	0.4
Raster angle	0/90	45/45

Table 1: Independent variables.

Research Design

The determination of number and value toward the variable level limits investigating the variables that may affect the process. In this research, the orthogonal array (orthogonal matrix) used was L4 (23) with three control factors and two levels for each control factor. Five replications were used in each combination. According to [11], the number of replication for a three-factor factorial is two. However, more than the minimum number of replication is preferable to be certain about the experimental error.

Implementation Stage

Before starting the printing process, it should prepare the specimen design using CAD. The design will be printed in the ASTM D790 bending test specimen. This design was chosen because it saves research costs by partnering with a group of pals who undertake flexural test research with the same materials and settings. The material dimensions of the ASTM D790 bending test specimen can be seen in **Figure 2**. The next step is to slice and set the parameters according to the combinations set in **Table 2**. After the printing is completed, the next process is to collect data using a digital caliper to measure each printed product's X, Y, and Z dimensions. Each dimension was measured by 5 mm apart. The measurement position of the printed object is presented in **Figure 2**.

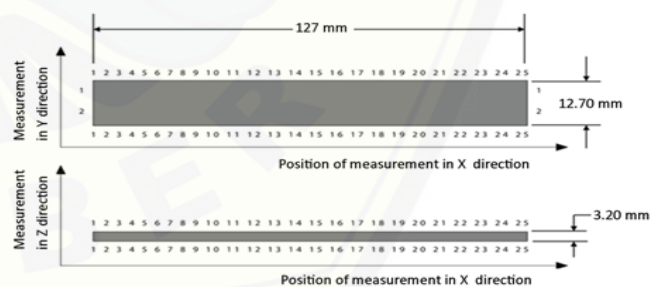


Figure 2: Specimen dimension and measurement position.

Then, the data were processed by using the Taguchi method with an S/N ratio. It aimed to determine the most optimal parameters. ANOVA (analysis of Variance) was employed to assess the contribution of each control parameter. The response applied is dimensional accuracy deviation; the smaller the deviation, the better it is. Therefore, the response characteristics used are "smaller is better".

Result and Discussion

The data result of the measurement will be compared

with the dimensions of the CAD design results that have been made (based on ASTM D790 standard dimension). The smaller the value of deviation from the nominal dimensions of the 3D printed product indicates the better dimensional accuracy in the experiment. It will take any data processing to obtain the deviation value for each replication. This was conducted three times the deviation value measurement results in each replication, such as on the X, Y, and Z-axis. Therefore, it is necessary to calculate the average for each replication to obtain one deviation value. The results of the average calculation of each replication can be seen in **Table 2**.

eSteel Filament Microstructure

eSteel filament is a filament made from a mixture of PLA and stainless steel. The eSteel filament mixture can be seen using a microscope with a magnification of 100 times. The microstructure of the eSteel filament was taken by cross-sectioned and longitudinal views presented in **Figures 3a and 3b**, respectively.

In **Figure 3** above, it can be seen that the composition transmission of the eSteel filament. The grains of stainless steel have various sizes. When it used a 3D printing machine with 220°C and 225°C temperatures, it did not significantly affect the microstructure of the eSteel filament either after or before the printing process. The results of the eSteel filament microstructure after 3D printing with a magnification of 100 times can be seen in **Figure 4**.

In **Figure 4** above, it can be concluded that after the 3D printing process was carried out by using eSteel filaments at 220°C and 225°C temperatures, it did not affect or even change the microstructure. In **Figure 4**, it can also be observed that stainless steel and PLA were not bonded perfectly (unblended) and only stuck to each other, even though the shape and size of the grains were permanent. The unchanged shape and size of stainless steel material at 220°C and 225°C temperatures can cause defects in dimensional accuracy. Whereby, during experimentation, we found the nozzle clogged with stainless steel grains during the progress of 3D printing.

Defects in the Specimens

Areas with Missing Material

Areas with missing material refer to an area that is empty or not filled by any materials. This defect was caused by the movement of the nozzle motion and the absence of fusion on stainless steel material during the printing process. The poor dimensional control happened because of the encounter of the interlayer, the differences in temperature, and the lack of

continuity. Therefore, it created unoccupied surfaces during printing. To overcome this defect, it can change the raster angle according to the shape as expected. This research is also supported by Günaydn K., who states that this kind of defect can be overcome by using better quality filaments to reduce its deficiency [12]. Areas with Missing Material can be seen in **Figure 5**.

Elephant's foot

The elephant's foot refers to the protrusion of the base model. Simply, it happens when it bends or curves at the bottom [13]. Elephant's foot defects occur because the speed of the nozzle movement was too fast when it reached the last point of a layer and moved to the other layer. Consequently, filaments placed in the exact space cause a curve. The way to overcome this defect is to determine the best nozzle speed because the fast pace on the nozzle may involve the filament layer control occurring in the same space, which causes a poor dimension. On the contrary, if the nozzle movement is too slow, it will pile up or create an accumulation. Elephant's foot defects can be seen in **Figure 6**.

Staircase effect

The staircase effect is a phenomenon associated with 3D printing when the layer marks are more clearly visible on the part's surface; it gives the perception of stairs. The

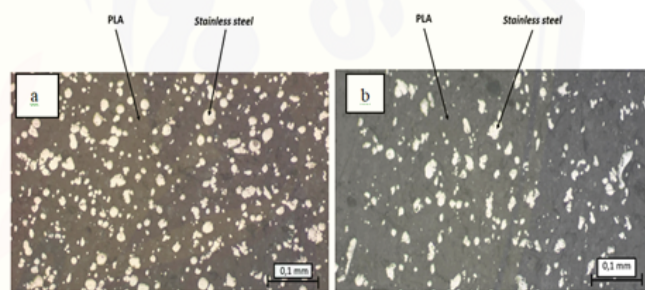


Figure 3: Microstructure of eSteel filament before extrusion with (a) cross-section view, and (b) longitudinal view.

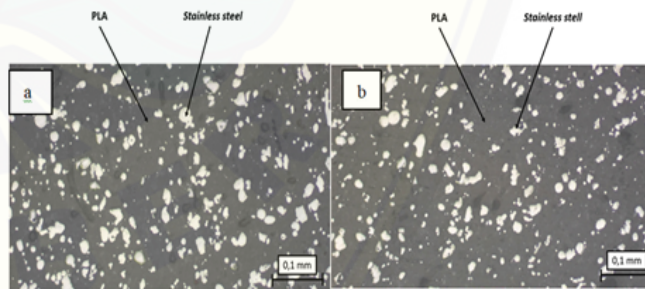


Figure 4: Printing results with extruder temperatures of (a) 220oC and (b) 225oC.

Combination	Variables/Parameters			Replication					Average	S/N Ratio (dB)
	Ext.Temp. (oC)	Layer height (mm)	Raster Angle (deg/deg)	I	II	III	IV	V		
1	2	3	4	5	6	7	8	9	10	11
1	220	0.3	0/90	0.18	0.23	0.21	0.23	0.28	0.23	12.8227
2	220	0.4	45/45	0.32	0.35	0.35	0.37	0.38	0.36	8.9762
3	225	0.3	45/45	0.36	0.37	0.36	0.37	0.36	0.36	8.8118
4	225	0.4	0/90	0.34	0.36	0.36	0.35	0.36	0.35	8.9968

Table 2: Result data of measurement.

layer height causes this defect, and the printing speed is too fast, so that it causes density between the layers and the filament control. Along with the discharge of a poor nozzle, it caused a staircase effect. This defect should reduce the height, layer thickness, and nozzle movement speed to obtain better dimensional control at the specimen angle. This investigation was supported by Yuan et al., who states that the staircase effect is a visual phenomenon that occurs in 3D printing, a defect that is caused by the differences in boundaries of adjacent layers during the printing of layers stacked on top of each other [14]. Staircase effect defects can be seen in **Figure 7**.



Figure 7: Staircase effect.

The authors have minimized some irregularity layers, such as the staircase. After several attempts during preliminary experiments, uniform layer were found at layer height of 0.3 mm and 0.4 mm. Therefore, those two values were implemented in the design of experiments. The appearance of layers with both layer heights is depicted in **Figure 8**.

The Calculation of S/N Ratio

The calculation of the S/N ratio is used to determine the quality of the product, so it can determine which information parameter is more influential on the response. The S/N ratio (Signal-to-Noise ratio) is the ratio between signal (controllable factor) and noise (uncontrollable factor). This research applied the quality characteristics of "the smaller is better" because the smaller the deviation, the better the quality of the product. The results of the S/N ratio can be seen in **Table 2** of the last column. The mean of means value

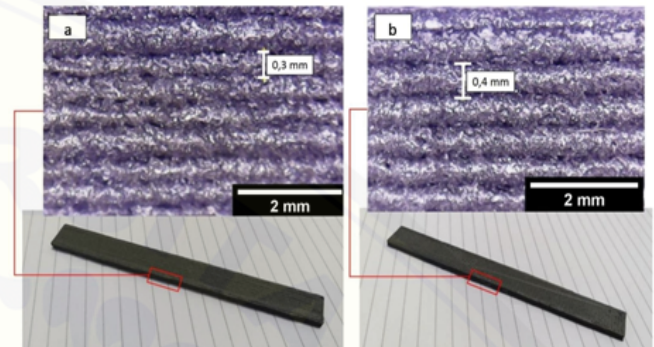


Figure 8: Conformity of printed layer height with the programmed one: (a) of 0.3 mm, and (b) of 0.4 mm.

is obtained from the average results of all replications in each experiment, and the calculation results can be seen in **Table 2**, column 10. To calculate S/N ratio using equation (1), while for means using equation (2).

S/N Ratio:

$$S/N = -10 \log \left(\sum \frac{Y^2}{n} \right) \quad (1)$$

Average means:

$$Means = \frac{1}{n} \sum_{i=1}^r Y_i \quad (2)$$

Optimal Variation Combination

With the Taguchi method, it is possible to obtain the optimal factors or a combination of factors. The optimal factors and levels are obtained from the highest S/N ratio. The calculation results of the average value of the S/N ratio on dimensional accuracy at various levels of the control factor are presented in **Figure 9**.

Calculation of ANOVA

Analysis of variance (ANOVA) is a calculation method that can quantitatively estimate the contribution of each factor to all response measurements. The analytical model used a two-way analysis of variance. The two-way analysis of the variance table consists of the calculation of degrees of freedom, the number of squares, the average number of squares, and the F-ratio. The ANOVA of this research was calculated based on "means" data. It is the following of a two-way ANOVA calculation of dimensional accuracy value. The

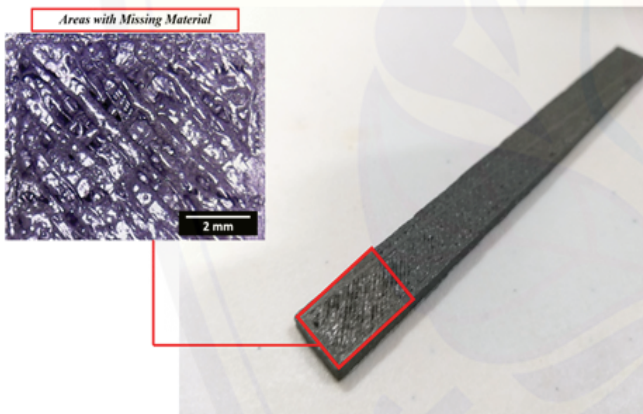


Figure 5: Areas with missing material.

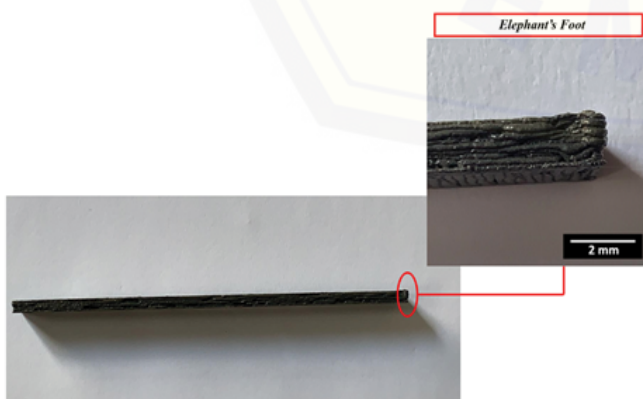


Figure 6: Elephant's foot.

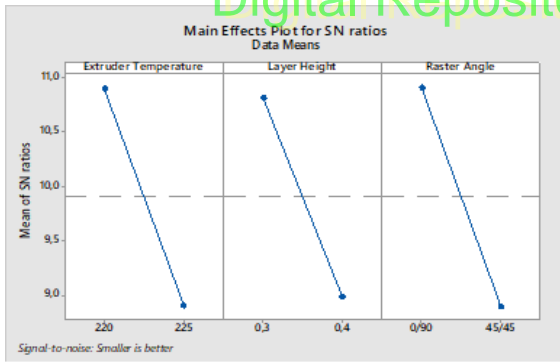


Figure 9: The plot of the S/N ratio average for every level of factors.

ANOVA is presented in **Table 3**. Calculation of the number of factor squares and the average of the factor squares using equations 3 and 4 while to find the residual error value using equation 5 and F-count using equation 6.

$$S_A = \frac{[TotalA_1]^2}{n_1} + \frac{[TotalA_2]^2}{n_2} + \frac{[TotalA_3]^2}{n_3} + \frac{[TotalA_4]^2}{n_1 + n_2 + n_3} \quad (3)$$

$$MSA = SS'A / DoF'A \quad (4)$$

$$Fe = (\text{total DoF}) - (\text{Total all factors DoF}) \quad (5)$$

Description:

$$F\text{-count} = MSA / MS'E \quad (6)$$

While the calculation of the percentage contribution using Equations 5 and 6. The results of the calculation of the percentage contribution can be seen in **Table 4**.

$$SS'A = SSA - MSe (DKA) \quad (7)$$

$$\rho A = SS'A / SS'T \times 100\% \quad (8)$$

Percent Contribution

Percent contribution arises from how much of the control parameter affects the response. The total variation can be reduced by controlling the high number of contributing factors to improve the process or product performance. The results of the percent contribution calculation can be seen in **Table 4**.

Discussion of Parameter Effect

The Effect of Raster Angle Parameter

Tontowi et al. stated that raster angle is an important parameter that affects the dimensional error [15]. That statement is also in line with this research. In this research, the contribution of raster angle to the dimensional accuracy of 3D printed products became the highest contribution than other factors, as presented in **Table 4**. above, at 32.09%. The most optimal raster angle belongs to raster angle level 1, which is 0/900. The deviation value of the 0/900 raster angle is smaller because the movement of the filament angle on the Y-axis at the 0/900 raster angle is better. Therefore it resulted in the best dimensional control. The dimensional control in the filament filling process only moves at a filling angle of 0° and 90°, which means it moves perpendicular to the Y-axis. Unlike a raster angle of 45/450, the filament angle of 45° on the nozzle has to proceed with a 450, which creates a slope that causes poor dimensional control.

The Effect of Extruder Temperature Parameter

In this research, the effect of the extruder temperature parameter has the second-highest percentage contribution value after the raster angle parameter, as presented in **Table 4** above. The percentage contribution to the effect of extruder temperature is 31.72%. The most optimal extruder temperature parameter is at level 1 under a temperature of 220 OC. It is classified as a quiet deviation because the higher the extruder temperature, the test will possibly process shrinkage and bending. At the same time, it may decrease the dimensional accuracy. This research is in accordance with the investigation conducted by Bahr et al. and Syrlybayev et al. who stated that the higher the temperature, the component would possibly shrink and risk toward product dimension [16-17].

The Effect of Layer Height Parameters

The layer height parameter of the 3D printing process is handy for determining the thickness and density of each layer. Sobron, et al. stated that the error value of 3D printing product specimen dimensional accuracy was due to the thickness of the layer [18-19]. It happened because a high layer height will produce a poor density among layers. In this research, the contribution of layer height to the dimensional accuracy of 3D printed products has the most negligible percentage contribution among other factors, as presented in **Table 4** above. It is 25.53%. The most optimal layer height parameter to produce good dimensional accuracy belongs to layer height level 1 with a layer thickness of 0.3 mm or the lower layer height. It produced an excellent layer density with a thickness of 0.3 mm, obtaining a flat and better surface.

Discussion of Flexural Strength

To complete discussion, the following section presents each specimen's bending test results, with only short discussion. The bending strength of the specimen is about the same at a maximum of 38 MPa, except for the combination 3, which results in lower stress at about 35 MPa. The flexural strength of pure PLA from manufacturer (of non 3D printing product) is 82.5 MPa [20]. The strain is relatively the same, regardless of the variations of the parameters. In the context of the application of 3D printers for prototyping, dimensional accuracy is more important than mechanical properties. In contrast, mechanical properties should be the premier consideration for functional application. Which mechanical properties will be used depends on the load or forces that work of the component.

The flexural strength resulted in this research is much lower than using pure PLA; it was 43.9 MPa and 43.8 MPa when applying layer thickness of 0.3 mm and 0.4 mm, respectively [21]. Other researchers have found that the flexural strength of 3D printed PLA was influenced by variation of infill density, infill angle, and infill speed; it was much lower between 5.53 MPa to 14.14 MPa [22]. The metal content in PLA may decrease flexural strength in comparison to pure PLA. By mixing bronze in PLA, the flexural strength of 3D printed specimens decreased from 78.45 MPa up to 41.69 MPa using a thickness layer of 0.4 mm [23].

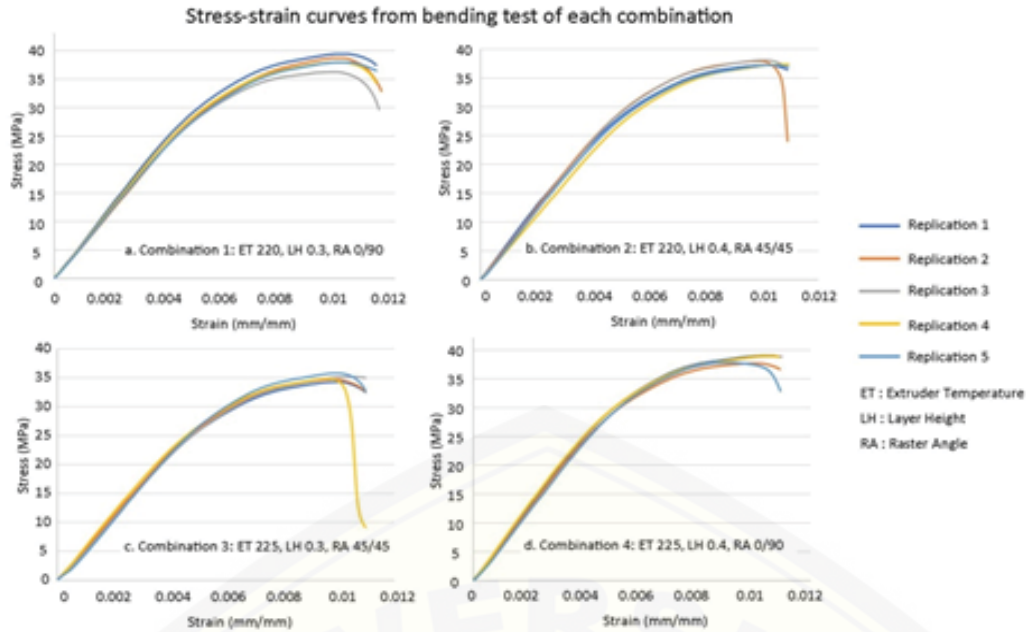


Figure 10: Stress-strain curves of each combination parameters.

Control Factors	DoF	SS	MS	F	P
Extruder Temperature	1	0.02312	0.02312	47.6137	Significant
Layer Height	1	0.018605	0.018605	38.3154	Significant
Raster Angle	1	0.0233928	0.0233928	48.1755	Significant
Error	16	0.0077692	0.000485575		
Total	19	0.072887			

Table 3: ANOVA table of control factors.

Control factors	Percent contribution (ρ)
Extruder Temperature	31,72%
Layer Height	25,53%
Raster Angle	32,09%
Error	10,66%
Total	100%

Table 4: Percent contribution of each factor:

Conclusion

The conclusion of the experimental results and analysis of the calculation of the Taguchi method concerning the effect of the extruder temperature, layer height, and raster angle parameters on the dimensional accuracy of 3D printed products with eSteel filament is as follows:

1. The most contributing factors to 3D printed products' dimensional accuracy are raster angle layer height and extruder with the contribution of 32.09%, 25.53, and 31.72%, respectively.
2. The combination of factors or parameters that can produce good dimensional accuracy is at extruder temperature of 220°C, a layer height of 0.3 mm, and a raster angle of 0°/90°.

Acknowledgment

This research was supported by the Research and Community Development Bureau of Universitas Jember through Post-Doctorate research grant scheme contract

number: 3473/UN25.3.1/LT/2020. We also thank Mas Oki Pranajaya, the technician of Mechanical Design Laboratory.

References

1. Gibson I and Rosen D. Additive Manufacturing Technologies. New York: Springer. 2015.
2. Murugan R, Mitilesh RN, Singamneni S. Influence of Process Parameters on The Mechanical Behaviour and Processing Time of 3D Printing. Int J Mod Manuf Technol. 2018;10:69-75.
3. Shazreen Kassim NS, Ibrahim M. Dimensional Accuracy Analysis for Desktop 3D Printers for Fused Deposition Modeling (FDM). Int J Mech Prod Eng. 2017;5:112-115.
4. Salmi M. Additive Manufacturing Processes in Medical Applications. Materials (Basel). 2021;14:1-16.
5. Jun W. Rapid Development of Dual Porous Poly (Lactic Acid) Foam using Fused Deposition Modeling (FDM) 3D Printing for Medical Scaffold Application. Mater Sci Eng. 2020;10:1-9.
6. Buchanan C, Gardner L. Metal 3D Printing in Construction: A Review of Methods, Research, Applications, Opportunities and Challenges. Eng Struct. 2019;180:332-348.
7. Schmutzler C, Zimmermann A, Zaeh MF. Compensating Warpage of 3D Printed Parts Using Free-form Deformation. Procedia CIRP. 2016;41: 1017-1022.

8. Solomon J, Sevel P, Gunasekaran J. Materials Today: Proceedings: A Review on The Various Processing Parameters in FDM. 2020; 10-15.
9. Rajpurohit S and Dave H. Tensile Properties of 3D Printed PLA under Unidirectional and Bidirectional Raster Angle: A Comparative Study. Int J Mater Metall Eng. 2018;12:6-11.
10. Sakthivel N, Bramsch J, Voung P, et al. Investigation of 3D-Printed PLA-stainless-steel Polymeric Composite through fused Deposition Modelling-Based Additive Manufacturing Process for Biomedical Applications. Med Devices Sensors. 2020;3: 1-21, 2020.
11. Krishnaiah K and Shahabudeen P. Applied Design of Experiments and Taguchi Method. New Delhi: PHI Learning Private Limited. 2012.
12. Gunaydin H, Kadir, Türkmen S. Common FDM 3D Printing Defects. Int Congr 3D Print. Additive Manuf Technol. 2018: 1-8.
13. Gunaydin H, Kadir, Türkmen S. Common FDM 3D Printing Defects. Int Congr 3D Print. Additive Manuf Technol. 2018:1-8.
14. Yuan J, Chen C, Yao D, et al. 3D Printing of Oil Paintings based on Material Jetting and Its Reduction of Staircase Effect. Polymers. 2020;12:1-12.
15. TAE, RL, ERV, et al. Optimization of 3D-Printer Process Parameters for Improving Quality of Polylactic Acid Printed Part. Int J Eng Technol. 2017;9:589-600.
16. Bähr F and Westkämper E. Correlations between Influencing Parameters and Quality Properties of Components Produced by Fused Deposition Modeling. Procedia CIRP. 2018;72:1214-1219, 2018.
17. Syrlybayev D, Perveen A, Talamona D. Fused Deposition Modelling: Effect of Extrusion Temperature on The Accuracy of Print. Mater Today Proc. 2023;44:832-837.
18. Lubis S. Pengaruh Orientasi Objek Pada Proses 3D Printing Bahan Polymer PLA Dan ABS Terhadap Keakuratan Tarik Dan Ketelitian Dimensi Produk. 2016:27-35.
19. Bual GS and Kumar P. Methods to Improve Surface Finish of Parts Produced by Fused Deposition Modeling. Manuf Sci Technol. 2014;2:51-55.
20. Reverte JM, Caminero MA, Chacon JM, et al. Mechanical and Geometric Performance of PLA-based Polymne Composite Processed by The Fused Filament Fabrication Additive Manufacturing Technique. Materials. 2020;13:3-16.
21. Nugroho A, Ardiansyah R, Rusita L, et al. Effect of Layer Thickness on Flexural Properties of PLA (PolyLactid Acid) by 3D Printing. J Phys Conf Ser. 2018;1130.
22. Kumar S, Singh R, Singh TP, et al. On Flexural and Pull Out Properties of 3D Printed PLA based Hybrid Composite Matrix. Mater Res Express. 2020;7.
23. Aveen KP, Vishwanath Bhajathari F, and Jambagi SC. 3D Printing & Mechanical Characteristion of Polylactic Acid and Bronze Filled Polylactic Acid Components. IOP Conf Ser Mater Sci Eng. 2018;376.

Copyright: © 2021 All copyrights are reserved by Mahros Darsin, published by Coalesce Research Group. This This work is licensed under the terms of the Creative Commons Attribution License, which permits unrestricted use, distribution and reproduction in any medium, provided the original author and source are credited.

Citation: Darsin M, Mahardika NA, Jatisukamto G, et al. Effect of 3D Printing Parameters on Dimensional Accuracy Using eSteel Filaments. J 3D Print Addit Manuf. 2021;1:1-7